Acta Oceanol. Sin., 2019, Vol. 38, No. 11, P. 91–98
https://doi.org/10.1007/s13131-019-1501-8
http://www.hyxb.org.cn
E-mail: hyxbe@263.net

Geotechnical properties and stability of the submarine canyon in the northern South China Sea

Jie Liu[1, 2*], Lejun Liu[3], Ping Li[1, 2*], Shan Gao[1, 2], Wei Gao[1, 2], Yuanqin Xu[1, 2]

[1] Key Laboratory of Marine Sedimentology and Environmental Geology, First Institute of Oceanography, Ministry of Natural Resources, Qingdao 266061, China

[2] Laboratory for Marine Geology, Pilot National Laboratory for Marine Science and Technology (Qingdao), Qingdao 266237, China

[3] Marine Engineering Environment & Geomatic Center, First Institute of Oceanography, Ministry of Natural Resources, Qingdao 266061, China

Received 12 November 2018; accepted 24 December 2018

Abstract

The upper part of the continental slope in the northern South China Sea is prone to submarine landslide disasters, especially in submarine canyons. This work studies borehole sediments, discusses geotechnical properties of sediments, and evaluates sediment stability in the study area. The results show that sediment shear strength increases with increasing depth, with good linear correlation. Variations in shear strength of sediments with burial depth have a significantly greater rate of change in the canyon head and middle part than those in the canyon bottom. For sediments at the same burial depth, shear strength gradually increased and then decreased from the head to the bottom of the canyon, and has no obvious correlation with the slope angle of the sampling site. Under static conditions, the critical equilibrium slope angle of the sediments in the middle part of the canyon is 10° to 12°, and the critical slope angle in the head and the bottom of the canyon is 7°. The results indicate that potential landslide hazard areas are mainly distributed in distinct spots or narrow strips on the canyon walls where there are high slope angles.

Key words: shear strength, slope stability analysis, submarine canyons, northern South China Sea

Citation: Liu Jie, Liu Lejun, Li Ping, Gao Shan, Gao Wei, Xu Yuanqin. 2019. Geotechnical properties and stability of the submarine canyon in the northern South China Sea. Acta Oceanologica Sinica, 38(11): 91–98, doi: 10.1007/s13131-019-1501-8

1 Introduction

Oil and gas exploitation is gradually advancing to deep water, with improvements in exploration and development technology. Deep water oil and gas resources constitute an important part of the growth in reserves (Wang et al., 2010; Thibodeaux et al., 2011). The International Energy Agency's world energy report in 2012 (IEA-WEO 2012) pointed out that the proportion of offshore oil production is expected to reach 35% in 2050, half of which is in deep water. With the experimental exploration and exploitation of natural gas hydrates, the development of deep water seabed resources has become a common goal of maritime countries around the world. However, compared with continental or shallow water oil and gas production, deep-water oil and gas development involves more risks and challenges (Randolph et al., 2011), especially in deep water area with complex terrain, where it is especially prone to geological hazards. Deep-water geological hazards are one of the biggest challenges in geoscience research. Their scale and influence are far beyond that of hazards on land and offshore. The volume of a large-scale sediment transport in turbidity current exceeds the sum of sediments that are discharged to the sea each year by all the rivers in the world (Talling et al., 2007). Existing projects demonstrate that almost all deep-water oil and gas resource development areas are affected by geological disasters to various degrees. One problem that needs attention is the instability of submarine slopes. This instability may cause submarine landslides and turbidity currents, which can destroy deep-water oil and gas exploitation infrastructure (Randolph et al., 2010; Krastel et al., 2014; Yuan et al., 2015).

The South China Sea is the southernmost marginal sea of the eastern Asia. The northern South China Sea is a passive continental margin and contains a series of submarine canyons. This area is rich in oil and gas resources, but also prone to submarine landslide disaster (Wu et al., 2011; Guan et al., 2014; He et al., 2014), especially in canyons on the upper part of the slope (Liu et al., 2014; Xiu et al., 2015). This paper studies borehole sediment cores from the continental slope of the northern South China Sea, discusses engineering geology properties of sediments, and evaluates sediment stability in the study area. It is important to understand the engineering geology characteristics of sediments, and safeguard the development of deep-water oil and gas exploitation.

2 Geological setting

The northern continental slope of the South China Sea ex-

Foundation item: The National Natural Science Foundation of China under contract No. 41706065; the National Program on Global Change and Air-Sea Interaction of China under contract No. GASI-GEOGE-05; the Special Fund of Chinese Central Government for Basic Scientific Research Operations in Commonweal Research Institutes under contract No. 2015G08; the NSFC-Shandong Joint Fund for Marine Science Research Centers of China under contract No. U1606401.
*Corresponding authors, E-mail: liujie@fio.org.cn; liping@fio.org.cn

tends northeast from east of the Xisha trough in the west to southeast of Taiwan in the east, following the contours of the southern China coast (Chen et al., 2013). It is approximately 900 km in length, and 143 km to 342 km in width. The submarine topography fluctuates greatly, generally tilted from the Northwest to Southeast. A series of canyons at different scales have developed in the area, including southeast of Hainan Island, at the mouth of the Zhujiang (Pearl) River Estuary, offshore of the Dongsha Islands, and Peng-hu and Kao-ping Submarine Canyons in the southwest of Taiwan Island (Ding et al., 2013). Below the slope is the continental apron, above which there are about 150 m to 250 m high hillocks or deep-sea fans. Seamounts in the deep-sea basin are usually 600 m to 800 m higher than the adjacent seabed. According to the topography, the northern continental slope of the South China Sea can be divided into three parts: the upper slope, with slope angels of 1° to 3°, and up to 4.5° south of the Taiwan shoal; the lower slope with slope angels of 2° to 4°, with the continental apron found at its junction with the deep sea basin (Xie, 1983); and the middle slope with notable terrain features, such as three-level gradual terraces.

The research area ranges from 114.5° to 116°E, and 19° to 20.25°N. This area contains the Liwan 3–1 gas field, Liuhua 34–2 gas field, and Liuhua 29–2 gas field, all of which are under construction.

3 Data and methods

In 2014 and 2015, we obtained 7 borehole samples in the study area. The locations of the samples are shown in Fig. 1, and the sampling depths are between 600 m and 1 700 m. Drilling was carried out by Ship 708 of the China National Offshore Oil Corporation (CNOOC). The volume weight (density), water content, and undrained shear strength of the sediment samples were tested. The cutting-ring method was used in the measurement of volume weight; water content was tested by the gravimetric method; and undrained shear strength was obtained by the electric cross plate method. The water depth and topography of the study area were obtained from multibeam sonar, autonomous underwater vehicle (AUV) deep tow multibeam echo-sounder, and seismic data inversion (Chen et al., 2015).

4 Results

4.1 *Physical and mechanical properties*

Change curves of water content and shear strength with burial depth were plotted for each borehole (Fig. 2). The boreholes are distributed from top to bottom along the canyon, and water depth increases gradually. However, because of their different locations in the canyon, the slope angles of the boreholes vary widely. In all boreholes, water content decreases with increasing burial depth. In shallow buried sediments, water content decreases rapidly with increasing burial depth; the greater the burial depth, the smaller the decrease in sediment water content. Borehole D03 has an abnormality from 0 to 5 m, where water content increases with the increasing burial depth. This may be attributed to the rapid accumulation of sediments at this location, and the lower sediments have not yet drained for consolidation. A gradual increase of sediment water content at the same burial depth is seen from top to bottom of the canyon. Taking surface sediments as an example, sediment water content increases from the canyon head (water depth: 600 m) at 60%, the middle canyon (water depth: 700 m to 1 200 m) at about 100%, and to 150% at the canyon bottom (water depth: 1 700 m).

Sediment shear strength increases linearly with burial depth in each borehole. The change rates in the canyon head and middle are significantly greater than those in the canyon bottom. Taking the burial depth of sediments with shear strength of 25 kPa as an example, in Borehole D01 at the canyon head that burial depth is 23 m; in other boreholes the burial depth increases from 15 m to 40 m with increasing water depth, indicative of a gradual increase. In addition, the shear strength of the sediments and the slope gradient of the drilling locations are not relevant; D01 and D02 holes located in the upper area of the canyon with minimum gradient have relatively high shear strength and low water content, while D06 and D07 holes located in the lower canyon area with similar gradients have low shear strength and high water content.

4.2 *Shear strength*

As shown in Fig. 2, sediment shear strength increases gradually with burial depth, and shear strengths at shallow burial

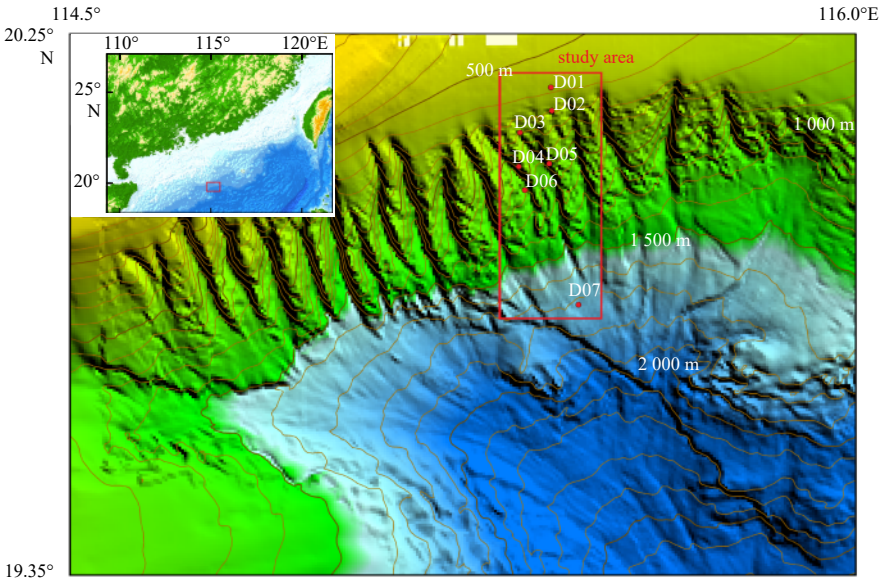

Fig. 1. Bathymetric map and the sampling locations.

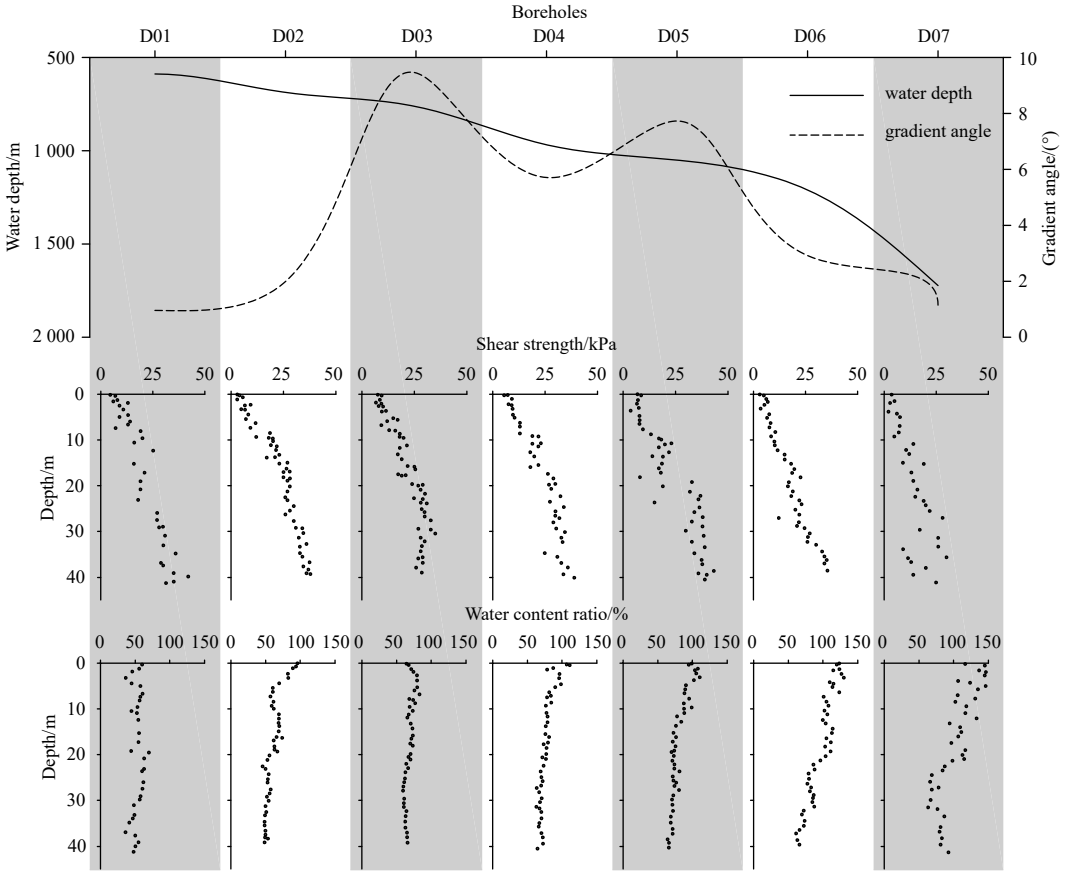

Fig. 2. Water content and shear strength with burial depth for each borehole.

depths are relatively concentrated, in the range of 0 kPa to 10 kPa. With increasing depth, shear strengths in different boreholes at the same burial depth have a greater range. To better understand the variations characteristics and their causes, this paper makes a preliminary classification of the water depth characteristics of the locations where each borehole was drilled, and scatter plots were created for sediment shear strength with burial depth (Fig. 3). Sediment shear strength and burial depth have a better linear correlation after classification according to the water depth of boreholes. The correlation coefficient of sediment shear strength and burial depth for all boreholes classified according to water depth is greater than 0.880, except for that of Borehole D07 located in the canyon bottom, which is 0.771. This further indicates that the vertical variations in sediment shear strength in the studied boreholes are closely related to water depth, but not closely related to the slope gradient. The sediment shear strength in D07 is obviously lower than that in other boreholes. In Borehole D07, shear strength of the surface sediments is only 4.8 kPa, and shear strength at 40 m burial depth is only about 30 kPa. The change rate of shear strength with burial depth is only 0.467 kPa/m, while the change rate in the canyon head and middle areas is 0.70 kPa/m to 0.85 kPa/m. Compared with sediments at the bottom of the canyon, sediments in the head and middle of the canyon have a significantly lower water content but higher shear strength.

To better understand variations in shear strength with burial depth for boreholes in different water depths, a trend line distribution characteristics graph of shear strength with burial depth in different water depths is shown in Fig. 4. Shear strength in the Borehole D07 at the bottom of the canyon is significantly smaller than that in the head and the middle part of the canyon. The physical and mechanical properties are characterized by high water content, high void ratio, low volume weight, and underconsolidation. In addition, the change rate of shear strength with burial depth for other water depths in the study area is small, and the trend line gradient for each borehole is basically the same, which is between 0.704 and 0.847. Only the shear strengths of surface sediments are different, at 3.3 kPa to 9.0 kPa. For sediments at the same burial depth, shear strength increases first and then decreases as water depth increases from the head to the bottom of the canyon.

4.3 *Stability evaluation of sediments*

The regional stability of submarine sediments in the study area was evaluated quantitatively with the limit equilibrium method (Gu, 1996; Brand et al., 2003; Li et al., 2017). The stability of an infinite slope is studied quantitatively with the safety factor F_s. The formula is as follows:

$$F_s = \frac{c' + r'Z\cos^2\alpha\left(1 - \frac{r}{r'}a\tan\alpha - \frac{U}{r'Z\cos^2\alpha}\right)\tan\varphi'}{r'Z\sin\alpha\cos\alpha\left(1 + \frac{r}{r'}\frac{a}{\tan\alpha}\right)},$$

where r and r' are the volume weight and effective gravity of the sediments, respectively, Z is the burial depth of the sliding surface, α is the slope angle, φ' is the internal friction angle, c' is the cohesion force, U is the pore water pressure, and a is the acceleration of the earthquake. In the case of no seismic load, a=0 in the above formula.

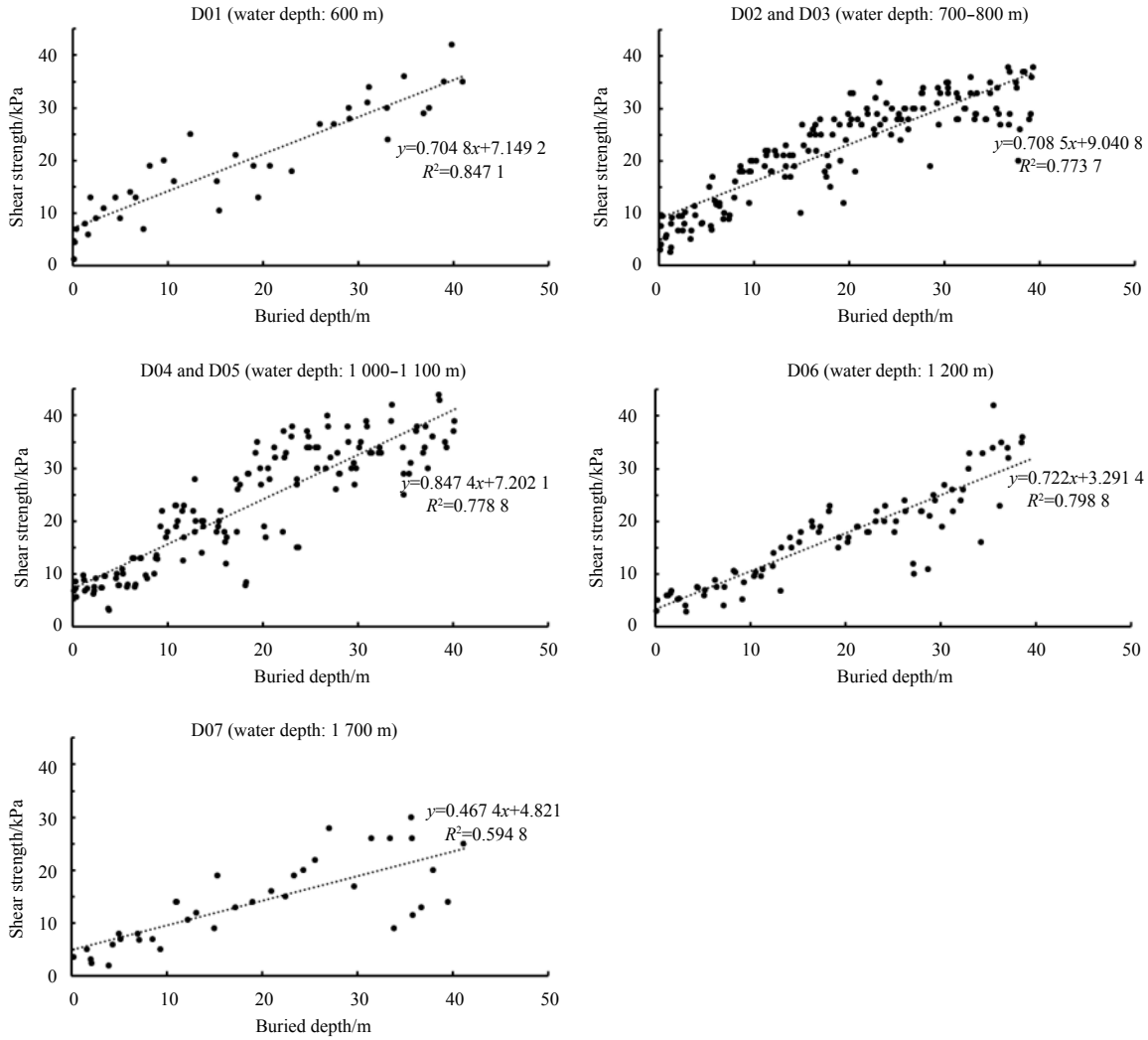

Fig. 3. Correlation scatter plot of the shear strength and buried depth.

Sediment stability was evaluated using the infinite slope limit equilibrium method under static conditions. Sediment shear strength is obtained by calculation from the data shown in Fig. 4. The effective gravity is obtained using the average value of sediment in each borehole. The stability of sediments at slopes of 2.5°, 5.0°, 7.5° and 10° is quantitatively evaluated by calculating the safety factor for different burial depths. The variations of safety factor with burial depth in Borehole D01 under different slope conditions are shown in Fig. 5 as an example. For a given slope angle, with increasing burial depth of a potential sliding surface, sediment stability decreases gradually, with an obvious power function relationship between them. For sediments with the same geotechnical properties and different slope angles, the safety factor at the same burial depth decreases gradually with increasing slope angles, and the rate of decrease slows significantly. After calculating the variations in safety factor under different slope angles, the slope angle for sediments in the critical equilib-

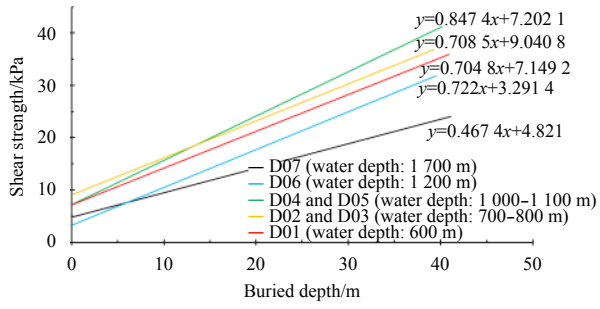

Fig. 4. Variations of sediment shear strength with burial depth for boreholes in different water depths.

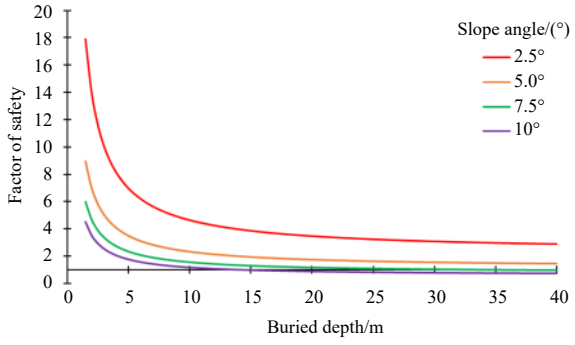

Fig. 5. Variations in safety factors under different slope angles and burial depths in Borehole D01.

rium state under static conditions is calculated by setting F_s=1. Safety factors for submarine slopes at different water depths and critical equilibrium angles are shown in Table 1. Shear strength varies with water depths in the middle canyon, but due to the good correlation between sediment volume weight and shear strength in each borehole, the critical equilibrium slope angles obtained do not differ much, and are between 10° and 12°. Shear strengths at the head and bottom of the canyon also differ. However, the critical equilibrium slope angles of sediments in these areas are both at 7°, due to the differences in the sediment volume weight.

Table 1. Safety factors for submarine slopes at different water depths and slope angles

Water depth of the boreholes/m	Safety factor				Critical equilibrium angle
	2.5°	5.0°	7.5°	10°	
600	2.894	1.448	0.967	0.727	7.2°
700–800	3.895	1.949	1.302	0.978	9.7°
1 000–1 100	4.711	2.358	1.574	1.183	11.7°
1 200	4.609	2.307	1.540	1.158	11.6°
1 700	2.696	1.349	0.901	0.677	6.7°

4.4 *Evaluation of regional stability*

Using the critical slope angle of sediments in different regions under limit equilibrium conditions, overall sediment stability in the study area is evaluated. The study area can be divided into three regions. Among them, the critical slope angle of sediments in the head and bottom of the canyon is 7°, and the critical slope angle in the middle part of the canyon is 10°. The stability of sediments in the study area can be evaluated by identifying potential landslide hazard areas from the topography, when the canyon head and bottom slope angles are greater than 7°, or the middle canyon slope angle is greater than 10°. A map of potential landslide hazard areas is shown in Fig. 6. Potential landslide hazard areas are mainly distributed on the canyon walls in areas with high slope angles. Xu et al. (2013) reported on turbidity currents resulting from local canyon wall slumping in a relatively big submarine canyon, indicating that frequent occurrences, in both space and time, of small-scale turbidity currents could be an important mechanism to cascade sediments and other particles in a big submarine canyon. This is consistent with the findings of this work, that hazard areas were mainly located on the canyon walls. In the study area, the potential landslide hazard areas are distinct spots or narrow strips, which is consistent with the previous findings (Li et al., 2015).

5 Discussion

5.1 *Stability analysis under the earthquake effects*

According to the potential area divided by the seismic structure in the study area, and the attenuation law of ground motion parameters obtained from local seismic intensity data and strong shock records, seismic risk probability analysis shows that earthquake acceleration a with a 50-year exceedance probability of 10% is 0.040 g to 0.071 g (Fig. 7). This work set a as the maximum, 0.071 g, to be conservative in analyzing regional stability of the study area under earthquake effects.

Taking Borehole D01 as an example, variations in safety factor with different burial depths and slope angles are shown in Fig. 8. For a given slope angle, sediment stability decreases gradually as the burial depth of the potential sliding surface increases. For sediments with the same geotechnical properties and different slope angles, the safety factor at a given burial depth decreases gradually with increasing slope angle. Compared with static conditions, sediment stability under earthquake effects is significantly reduced, and the range of the potential landslide hazards in the study area is significantly increased. After calculating the sediment safety factor under different slope angles, the critical slope angle for sediments in the equilibrium state under earthquake effects is calculated by setting F_s=1. Safety factors for different slope angles and critical angles under earthquake effects at different water depths are shown in Table 2. The critical equilibrium slope angle in the middle of the canyon under earthquake effects is still greater than that in the canyon head and bottom, but is reduced from 10° to 12° under static conditions to 6° to 8°. The critical equilibrium slope angle of the canyon head and bottom is reduced from about 7° to about 3°. The data indicate that earthquakes have a significant influence on regional sediment stability, but landslides occur infrequently in the study area due to low seismic activity.

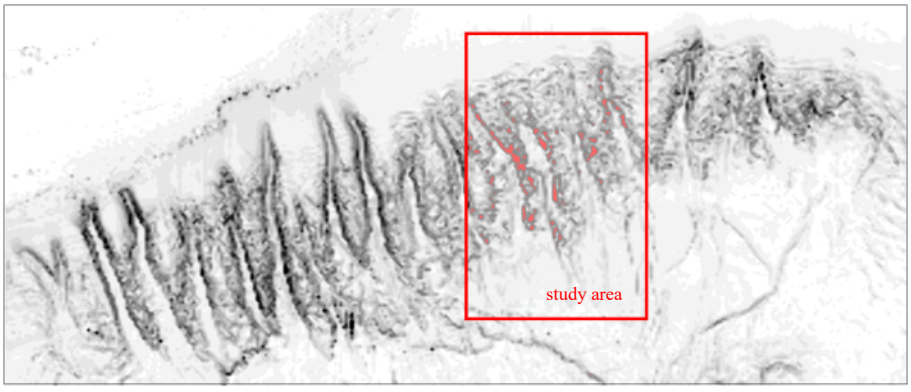

Fig. 6. Map of potential landslide hazard areas under static condition.

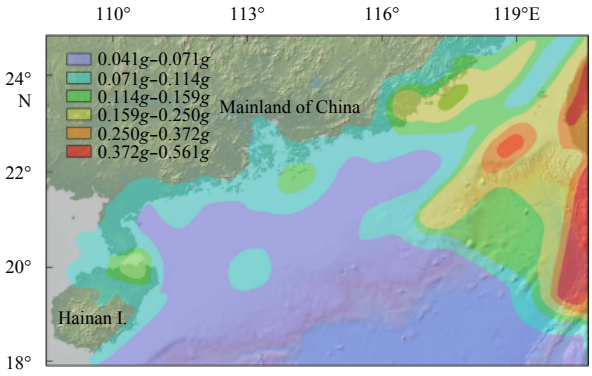

Fig. 7. Distribution map of peak ground accelerations in the northern South China Sea (modified from Chen et al. (2009); Hu et al. (2014))

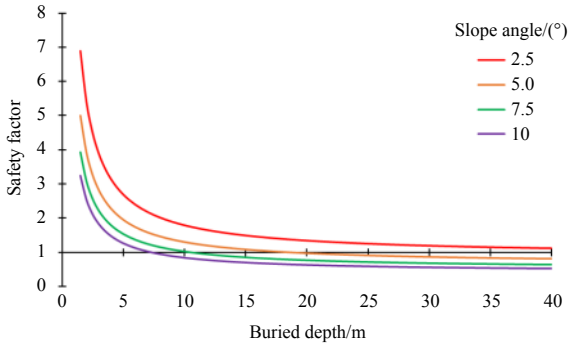

Fig. 8. Variations in safety factor at different slope angles and burial depths under earthquake effects for Borehole D01.

5.2 *Shear strength distribution analysis*

Under normal conditions, sediments are deposited and consolidated under gravity stress and overburden stress. Shear strength increases with increasing burial depth. But if discontinuities or landslides occur, the curves for shear strength with burial depth change with the variations in deposition processes. Borehole D01 is located in a flat area of the canyon head, where sediment has normal continuous deposition and compressive strength increases with increasing burial depth under gravity stress. Boreholes D02 and D04 are located in the middle of the canyon, where the slope is large and is prone to landslides. Landslides may occur after sediment deposition and consolidation, due to submarine currents and earthquakes. Surface sediments may collapse and be transported away, exposing the underlying sediments. Compared with the head of the canyon, sediment shear strength in this area is relatively high and water content is relatively low. Borehole D07 is located in the bottom of the canyon, changes in shear strength are not obvious with increasing burial depth. The change rate of shear strength is significantly lower than in other regions, and sediments are characterized by high water content and high compressibility. The bottom of the canyon is the sink for landslides. Large sediment volumes with high water content from landslides accumulate at the bottom of the canyon. Sediments are disturbed in the process of sliding, and lose their original physical and mechanical properties. Sediment shear strength increases and then decreases from the head to the bottom of the canyon area, while the trend of water content is the opposite, which is also indirect evidence of landslides in the study area.

The variations in sediment shear strength with burial depth from the head to the bottom of the canyon, reflect different sedimentary environments and processes in different areas. The variations of shear strength with burial depth are also indirect evidence of landslides.

5.3 *Scientific significance and application*

Gu (1996), Zhang and Luan (2012, 2013) evaluated sediment stability on the northern continental slope of the South China Sea. However, the data on physical and mechanical properties of sediments were limited due to the limited number of boreholes. The whole study area is represented by small numbers of boreholes, and there is no ability to differentiated sediment mechanical properties in the study area. The critical equilibrium slope angles of sediments in the research area under static conditions are calculated using the physical and mechanical data, but no similar calculations are done based on differences in sediment physical and mechanical properties at different slope locations and water depths.

The results of this work show that the physical and mechanical properties of sediments in different areas of the submarine canyon are very different. Taking the water content and sediment shear strength as an example, from the head to the bottom of the canyon, the shear strength gradually increases and then decreases with increasing water depth. The trend of water content is the opposite, but there is no significant correlation between sediment physical and mechanical properties and the slope angle at the sampling location.

Based on the infinite slope limit equilibrium method, the critical equilibrium slope angles of sediments in different areas of the canyon were calculated under static conditions. The results show that shear strength varies with water depth in the middle canyon area, but due to the good correlativity between sediment volume weight and shear strength in each borehole, the critical equilibrium slope angles among the boreholes do not differ much, and are between 10° and 12°. Shear strength at the head and bottom of the canyon differs more, but due to the differences in sediment volume weight, the critical equilibrium slope angles of the two areas are both about 7°. From these results, the study area is divided into three different areas. Regional sediment stability is evaluated according to the topography, and potential landslide hazard areas are identified where the canyon head and bottom slope angles are greater than 7°, or the middle

Table 2. Safety factors for submarine slopes under earthquake effects

Water depth of the boreholes/m	Safety factor				Critical equilibrium angle
	2.5°	5.0°	7.5°	10°	
600	1.112	0.806	0.633	0.523	3.2°
700–800	1.497	1.085	0.852	0.703	5.7°
1 000–1 100	1.811	1.312	1.031	0.851	7.8°
1 200	1.772	1.284	1.009	0.832	7.6°
1 700	1.036	0.751	0.589	0.487	2.7°

canyon slope angle is greater than 10°.

The results indicate that when evaluating the regional sediment stability in continental slope or canyon areas, physical and mechanical properties of the sediments should be studied first. When the physical and mechanical properties of sediments in different areas differ greatly, the study area should be divided, to calculate critical equilibrium slope angles in different subareas under static conditions.

5.4 *The representativeness of boreholes and the prospect*

The conventional method for research on submarine sediment stability is to collect enough boreholes samples to fully assess the potential hazards. Sufficient sampling can obtain the engineering geological parameters needed to assess the stability of the seabed in shallow water. It is impossible to get enough samples in deep waters, owing to such variables as the impacts of water depth, technology and cost. It is unrealistic to evaluate the physical and mechanical properties of sediments in the same way as in shallow waters. Usually, key sampling and evaluation of representative sedimentary profiles or potentially hazardous areas are performed. Although the causes and sedimentary environments of the canyons in the study area are basically the same, when the incomplete and discontinuous survey data must represent the whole, the geological parameters of important inflection points may be overlooked, which may lead to imperfect understanding of regional sediment stability.

Therefore, it is particularly important to explore an economic and feasible method for obtaining engineering geological parameters for comprehensive coverage of deep-water areas. Li et al. (2017) predicted potential landslide zones using seismic amplitude in Liwan gas field, northern South China Sea. However, the correlation between seismic amplitude and sediment shear strength is poor, due to few numbers of boreholes and less parameter variables. The evaluation of regional sediment stability may also be flawed, as the inversion obtained the average value of shear strength in sediments of 12 m depth. But the exploration is very meaningful. In the future, we can try to establish correlations among multiple parameters by collecting large amounts of physical and mechanical data for borehole sediments and corresponding seismic amplitude data. Using physical and mechanical properties of sediment from different areas, full coverage of the engineering geological characteristics of large deep-sea areas can be obtained quantitatively to evaluate the regional stability.

6 Conclusions

(1) There is good linear correlation between shear strength and burial depth of borehole sediments. The change rates of shear strength with burial depth in the canyon head and middle areas are 0.70 kPa/m to 0.85 kPa/m, and it is only 0.467 kPa/m in the bottom of the canyon.

(2) For sediments with the same burial depth, as the water depth increases, shear strength generally increases and then decreases, while the trend of water content is opposite. There is no significant correlation between the physical and mechanical properties of sediments and the slope angle of the borehole location.

(3) Under static conditions, the critical slope angle is between 10° and 12° in the middle of the canyon under limit equilibrium conditions, while the critical slope angle is around 7° in the head and bottom of the canyon. Potential landslide hazard areas are mainly distributed on the canyon walls, in distinct spots or narrow strips.

References

Brand J R, Lanier D L, Berger III W J, et al. 2003. Relationship between near seafloor seismic amplitude, impedance, and soil shear strength properties and use in prediction of shallow seated slope failure. In: Proceedings of 2003 Offshore Technology Conference. Houston, USA: OTC

Chen Renfa, Kang Ying, Huang Xinhui, et al. 2009. Seismic risk analysis in Northern South China Sea. South China Journal of Seismology (in Chinese), 29(4): 36–45

Chen Yilan, Liu Lejun, Liu Xiaoyu, et al. 2015. Seabed topographic survey technology in deep-sea oil and gas exploration. Hydrographic Surveying and Charting (in Chinese), 35(2): 18–22

Chen Duanxin, Wu Shiguo, Dong Dongdong, et al. 2013. Focused fluid flow in the Baiyun Sag, northern South China Sea: implications for the source of gas in hydrate reservoirs. Chinese Journal of Oceanology and Limnology, 31(1): 178–189, doi: 10.1007/s00343-013-2075-5

Ding Weiwei, Li Jiabiao, Li Jun, et al. 2013. Formation process and controlling factors of the Pearl River Canyon in the South China Sea. Journal of Tropical Oceanography (in Chinese), 32(6): 63–72

Gu Xiaoyun. 1996. Case study of clayey seabottom stability. Journal of Engineering Geology (in Chinese), 4(1): 32–38

Guan Jinan, Liang Deqing, Wan Lihua, et al. 2014. Analyses on dynamic methane hydrate accumulation simu-lation in Shenhu area of the northern South China Sea. Journal of Engineering Geology (in Chinese), 22(5): 997–1022

He Ye, Zhong Guangfa, Wang Liaoliang, et al. 2014. Characteristics and occurrence of submarine canyon-associated landslides in the middle of the northern continental slope, South China Sea. Marine and Petroleum Geology, 57: 546–560, doi: 10.1016/j.marpetgeo.2014.07.003

Hu Jinjun, Hao Yanchun, Xie Lili. 2014. Effects of potential earthquakes on construction and development in South China Sea region. China Earthquake Engineering Journal (in Chinese), 36(3): 616–621

Krastel S, Behrmann J H, Völker D, et al. 2014. Submarine mass movements and their consequences. Advances in Natural & Technological Hazards Research, 37(3): 517–524

Li Xishuang, Liu Lejun, Li Jiagang, et al. 2015. Mass movements in small canyons in the northeast of Baiyun deepwater area, north of the South China Sea. Acta Oceanologica Sinica, 34(8): 35–42, doi: 10.1007/s13131-015-0702-z

Li Xishuang, Liu Baohua, Liu Lejun, et al. 2017. Prediction for potential landslide zones using seismic amplitude in Liwan gas field, northern South China Sea. Journal of Ocean University of China, 16(6): 1035–1042, doi: 10.1007/s11802-017-3308-6

Liu Lejun, Fu Mingzuo, Li Jiagang, et al. 2014. Geologic hazards in the deep pipeline routing area of the Liwan 3-1 gas field in the South China Sea. Advances in Marine Science (in Chinese), 32(2): 162–174

Randolph M F, Gaudin C, Gourvenec S M, et al. 2011. Recent advances in offshore geotechnics for deep water oil and gas developments. Ocean Engineering, 38(7): 818–834, doi: 10.1016/j.oceaneng.2010.10.021

Randolph M F, Seo D, White D J. 2010. Parametric solutions for slide impact on pipelines. Journal of Geotechnical and Geoenvironmental Engineering, 136(7): 940–949, doi: 10.1061/(ASCE)GT.1943-5606.0000314

Talling P J, Amy L A, Wynn R B, et al. 2007. Evolution of turbidity currents deduced from extensive thin turbidites: Marnoso Arenacea Formation (Miocene), Italian Apennines. Journal of Sedimentary Research, 77(3): 172–196, doi: 10.2110/jsr.2007.018

Thibodeaux L J, Valsaraj K T, John V T, et al. 2011. Marine oil fate: knowledge gaps, basic research, and development needs; a perspective based on the deepwater horizon spill. Environmental Engineering Science, 28(2): 87–93, doi: 10.1089/ees.2010.0276

Wang Zhen, Chen Chuanying, Zhao Lin. 2010. Present situation and challenge of exploration and production for deep water oil and gas in the whole world. Sino-Global Energy (in Chinese), 15(1): 46–49

Wu Shiguo, Qin Zhiliang, Wang Dawei, et al. 2011. Seismic characteristics and triggering mechanism analysis of mass transport deposits in the northern continental slope of the South China Sea. Chinese Journal of Geophysics (in Chinese), 54(12): 3184–3195

Xie Yixuan. 1983. Bottom geomorphology of the northeastern South China Sea. Tropic Oceanology (in Chinese), 2(3): 182–190

Xiu Zongxiang, Liu Lejun, Xie Qiuhong, et al. 2015. Runout prediction and dynamic characteristic analysis of a potential submarine landslide in Liwan 3-1 gas field. Acta Oceanologica Sinica, 34(7): 116–122, doi: 10.1007/s13131-015-0697-2

Xu J P, Barry J P, Paull C K. 2013. Small-scale turbidity currents in a big submarine canyon. Geology, 41(2): 143–146, doi: 10.1130/G33727.1

Yuan Feng, Li Lingling, Guo Zhen, et al. 2015. Landslide impact on submarine pipelines: analytical and numerical analysis. Journal of Engineering Mechanics, 141(2): 04014109, doi: 10.1061/(ASCE)EM.1943-7889.0000826

Zhang Liang, Luan Xiwu. 2012. Quantitative analysis of submarine slope stability on the northern slope of the South China Sea. Progress in Geophysics (in Chinese), 27(4): 1443–1453

Zhang Liang, Luan Xiwu. 2013. Stability of submarine slopes in the northern South China Sea: a numerical approach. Chinese Journal of Oceanology and Limnology, 31(1): 146–158, doi: 10.1007/s00343-013-2060-z